Cell

Leading Edge
Primer

Metabolomics and Isotope Tracing

Cholsoon Jang,[1] Li Chen,[1] and Joshua D. Rabinowitz[1,*]
[1]Lewis Sigler Institute for Integrative Genomics and Department of Chemistry, Princeton University, Washington Rd, Princeton, NJ 08544, USA
*Correspondence: joshr@princeton.edu
https://doi.org/10.1016/j.cell.2018.03.055

Great strides have been made over the past decade toward comprehensive study of metabolism. Mass spectrometry (MS) has played a central role by enabling measurement of many metabolites simultaneously. Tracking metabolite labeling from stable isotope tracers can in addition reveal pathway activities. Here, we describe the basics of metabolite measurement by MS, including sample preparation, metabolomic analysis, and data interpretation. In addition, drawing on examples of successful experiments, we highlight the ways in which metabolomics and isotope tracing can illuminate biology.

Introduction

Since the discovery of DNA, biological research has steadily accelerated due to ever-increasing ability to control genes and their protein products. Against the backdrop of the revolutionary progress, metabolism research remained comparatively stagnant for many decades. The past decade, however, has seen a swell of interest. The ongoing epidemic of obesity and metabolic syndrome is one reason for this resurgence. Metabolism, however, plays a central role in all areas of biology, from ecology to bioengineering to cancer (Figure 1). Each of these areas is now being increasingly examined from a metabolic viewpoint. In such efforts, there is high value to taking a big-picture perspective. This is feasible due to advances in metabolite measurement technologies like NMR and mass spectrometry (MS) (Fiehn, 2002; Beckonert et al., 2007).

Measurement of metabolite concentrations by metabolomics, however, tells only half the story. Equally important is understanding pathway activity, which can be quantified in terms of material flow per unit time, i.e., metabolic flux (Sauer, 2006). Concentrations and fluxes do not reliably align. This is intuitive to drivers: although flux increases with car density until traffic slows, a high concentration of cars on the road does not reliably indicate high flux (Figure 2A). Similarly, in metabolism, metabolite build-up can occur not only due to increased production, but also due to decreased consumption. For example, when glucose is removed from yeast, glycolytic efflux drops sharply, leading to build-up of lower glycolytic intermediates even though pathway influx is decreased (Figure 2B, Lowry et al., 1971; Xu et al., 2012). Because metabolite levels and fluxes provide complementary information, metabolic understanding is best achieved by investigating both.

Unlike metabolites, fluxes are not physical entities that can be measured in a mass spectrometer. They can be inferred, however, through use of isotope tracers. Classical radioactive tracer studies laid the foundations for modern understanding of metabolism. Today, similar studies can be performed using MS or NMR to follow, broadly and quantitatively, the fate of non-radioactive stable isotope tracers. To quantitate fluxes at the systems level, copious tracer data are integrated using computational models. But without such computation, valuable biological insights can nevertheless be obtained by intuitive interpretation of isotope tracer experiments. Moreover, intuition can often be complemented by using equations to quantitate key fluxes or flux ratios. Such targeted isotope tracer methods are covered together with metabolomics here.

The Metabolome

Metabolites are produced and consumed by a network of coupled enzymatic reactions that converts incoming nutrients into usable energy and biomass. At steady state, the quantitative inflows and effluxes from each metabolite must balance (O'Brien et al., 2015). The scale of the metabolic network varies by organism from around 500 to a few thousand reactions and water-soluble metabolites. The structures of these metabolites are largely identical from bacteria to humans. This reflects the fact that all organisms need nucleotides, amino acids, and fatty acids to make DNA/RNA, proteins, and membranes. Nearly all make or consume glucose, with cellulose the most abundant biopolymer on earth. Accordingly, around 100 high-flux compounds are consistently major metabolome constituents: amino acids, nucleotides, and intermediates of glycolysis, the pentose phosphate pathway (PPP), and the TCA cycle.

In contrast to the finite core of metabolism, the full scope of small molecules in biological systems is vast. It includes other functionally important metabolites: enzyme activators and inhibitors; donors and regulators of macromolecule modifications (Table 1); signaling molecules including neurotransmitters and hormones; mediators of interspecies warfare like antibiotics; and structural and energy storage molecules such as lipids. Because lipids are so numerous and their properties are different from water-soluble metabolites, lipid measurement is its own 'omics field (lipidomics) (Wenk, 2010). In addition to endogenous metabolites, organisms that are higher on the food chain contain secondary metabolites made by other species. Human samples typically also contain drugs, artificial flavors, and other xenobiotics, as well as their metabolic byproducts.

Beyond known metabolites, there is substantial interest in the unknown metabolome. While the full set of genes and proteins in

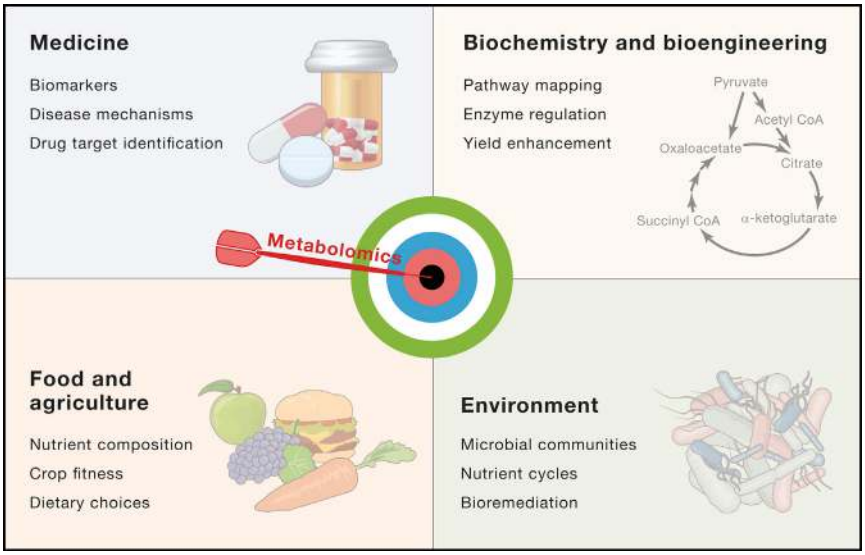

Figure 1. Applications of Metabolomics

an organism can be revealed by genome sequencing, the full set of metabolites remains ill-defined due to the catalytic potential of uncharacterized proteins, enzyme promiscuity, and the diversity of metabolic inputs coming from food. The observation that most peaks in mass-spectrometry-based metabolomics studies remain unidentified has increased interest in unknown metabolome (Domingo-Almenara et al., 2018), although many of these peaks are analytical artifacts (Mahieu and Patti, 2017). Nevertheless, new metabolites and reactions certainly remain to be discovered.

Metabolomics

Metabolomics, with or without isotope tracing, involves three basic steps: (1) sample preparation, (2) metabolome measurement, and (3) data analysis (Figure 3). While the measurement step involves the glamorous technology, sample preparation and data analysis are equally important.

Sample Preparation

Success in metabolomics starts with picking the right experiment. In this regard, we hope that readers will be motivated by some of the biological applications described below, as well as Table 2, which highlights many different isotope tracers and their utility. In this section, we focus on basic design issues in metabolomics studies, which apply across many applications.

Control of the nutrient environment is particularly important. For *in vivo* studies, this means close attention to feeding, fasting, and diet composition. For cell culture studies, it means special care in media selection and timing of media changes. Chemically defined media is generally preferred to complex biological media like lysogeny broth (LB). For mammalian cell culture, use of dialyzed fetal bovine serum, which is readily commercially available, avoids confounds due to serum metabolites.

For isotope tracer studies, it is often preferable to avoid metabolic perturbations when introducing the tracer, i.e., to maintain "metabolic steady state." This can be accomplished by switching into otherwise identical media with particular nutrient(s) changed from unlabeled to labeled form. Duration of labeling depends on the pathways of interest and whether aiming for dynamic or steady-state data. In cultured cells, steady-state labeling (i.e., "isotopic steady state") is typically achieved in glycolysis over ~10 min, the TCA cycle over ~2 hr, and nucleotides over ~24 hr. Very rapid sampling is required to capture glycolytic labeling dynamics (e.g., 10 s timescale), whereas TCA dynamics can be probed by sampling at time points like 15, 30, 60, and 120 min. One-day experiments are often convenient for collecting steady-state labeling data.

Another key issue is harvesting metabolites. This is a particular challenge for cells and tissues, as many important metabolites naturally turnover within seconds. Thus, obtaining an accurate metabolite profile requires stopping metabolic activity nearly instantaneously. This remains an area of active research. Typical approaches include freezing and/or enzyme denaturation (Figure 3). A variety of extraction and quenching protocols have been reported (Winder et al., 2008; Dietmair et al., 2010; Want et al., 2013). For cultured cells, a simple approach is to add cold organic solvent directly after media removal by

Table 1. Selected Examples of Metabolites Impacting Macromolecule Modifications

Modification	Principal targets	Metabolic substrate	Metabolic product or reaction inhibitor
Phosphorylation	Proteins	ATP	ADP
Acetylation	Proteins	Acetyl-CoA	CoA
Deacetylation	Proteins	NAD (sirtuins)	Nicotinamide (sirtuin inhibitor) Butyrate, 3-hydroxybutyrate (HDAC inhibitor)
Methylation	DNA, histones	S-adenosyl-methionine	S-adenosyl-homocysteine
Demethylation	DNA, histones	α-ketoglutarate, O_2	Succinate, fumarate, 2-hydroxyglutarate
GlcNAcylation	Proteins	UDP-N-acetylglucosamine	UDP
Acylation	Proteins	Acyl-CoA (e.g., palmitoyl-CoA)	CoA

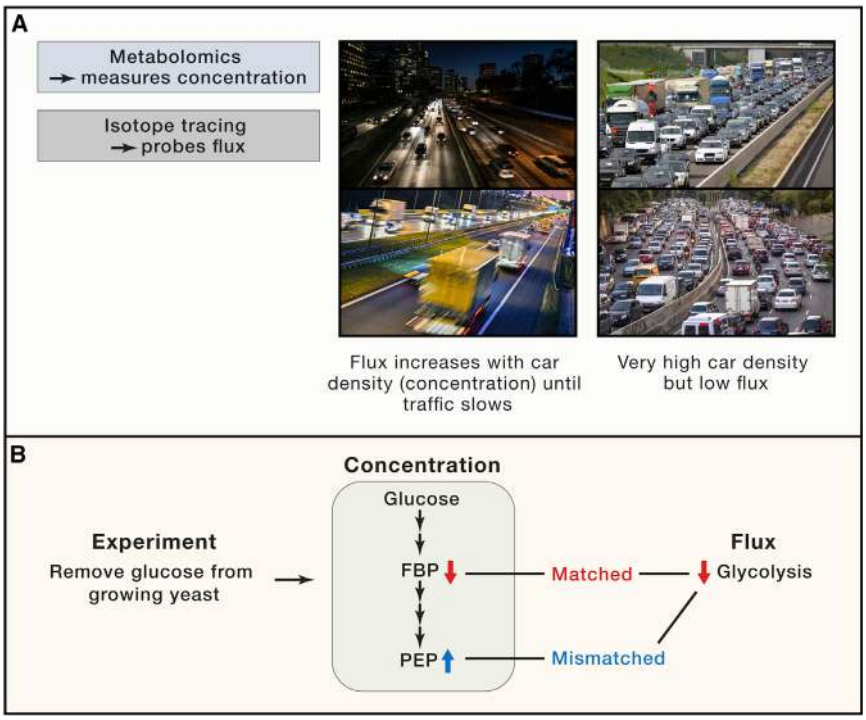

Figure 2. Metabolite Levels versus Metabolic Flux

(A) Concentration and flux are distinct properties. (B) Biological example of divergence between concentration and flux. Glucose removal decreases flux throughout glycolysis, but some glycolytic intermediates increase. FBP, fructose-1,6-bisphosphate; PEP, phosphoenolpyruvate.

aspiration (for adherent cells) or fast filtration (for non-adherent cells). The cold temperature quickly slows metabolism, and the organic solvent permanently denatures enzymes. Manipulations that may alter metabolism, such as pelleting or washing cells prior to quench metabolism, are best avoided (Wittmann et al., 2004).

For tissue specimens, it is most practical to freeze first and then extract. Quick freezing can be achieved by smashing tissue between liquid-nitrogen-temperature metal plates, a technique known as the Wollenberger clamp (Figure 3) (Wollenberger et al., 1960). Due to superior heat transfer, this results in substantially faster freezing than placing tissue pieces directly into liquid nitrogen. Tissues can then be stored at −80°C, pulverized by grinding, and extracted with cold organic solvent. Care must be taken to avoid metabolic alterations both before and during sampling. This is not straightforward, as anesthesia or euthanasia can each induce metabolic changes (Overmyer et al., 2015). Indeed, even the sight of an experimenter (or doctor) may induce a stress response that alters metabolism (Sorge et al., 2014).

Another complication is that organic solvent may not immediately stop enzymatic activity. Persistent catalytic activity is a particular problem for high-energy compounds like NADPH and ATP. The degradation products of these abundant metabolites are themselves biologically important metabolites, with even modest degradation of NADPH markedly increasing NADP and ATP markedly increasing ADP and AMP. For biologists interested in such compounds, we recommend extracting with a combination of organic solvent and acid, as the acid accelerates enzyme denaturation. Specifically, we find that a mixture of 40:40:20 acetonitrile:methanol:water with 0.1 M formic acid, followed by addition of bicarbonate a few minutes later to neutralize the samples, effectively captures these metabolites (Rabinowitz and Kimball, 2007; Lu et al., 2018). Further research is likely to yield yet better methods going forward.

The inherent challenges in metabolome sampling render confirmatory measurements valuable. For example, does a particular genetic perturbation produce the same metabolic changes in liver sampled both from anaesthetized and from euthanized mice? Alternatively, certain metabolites can be measured directly *in vivo*, e.g., using fluorescent reporters (Looger et al., 2005; Hung et al., 2011; Rogers and Church, 2016). At the same time, it is important to recognize that even imperfectly collected samples can yield valuable insights. Some delays in quenching typically occur during tissue sampling in clinical studies, but this is a reasonable trade-off for the benefits of human data.

MS

With an extract in hand, the challenge is to measure as many metabolites as possible, as accurately as possible. In the early days of metabolomics, one-dimensional proton NMR was commonly used to produce metabolome profiles. While peaks could be assigned to functional groups (e.g., CH_2 signal from fatty acid tails), most peaks reflected the integrated signals from multiple metabolites. These limitations have been partially resolved by multidimensional NMR (Larive et al., 2015; Markley et al., 2017), and NMR continues to play an important role in metabolomics due to its capacity for structure elucidation, *in vivo* metabolite measurement (Mancuso et al., 2004; Salamanca-Cardona et al., 2017), and universal detection (nearly every metabolite contains a proton and thus gives a proton NMR signal). Nevertheless, investigators are increasingly relying on MS due to its unmatched capability for detecting low-abundance metabolites without interference from closely related species (Figure 4).

This reflects the remarkable resolving power and sensitivity of modern mass spectrometers. In MS, resolving power is defined as the ratio m/Δm, where m is the analyte mass and Δm is the smallest mass difference that can be distinguished (Figure 4B). Achieving high resolution allows metabolites with small mass differences to be independently measured. For example, creatine ($C_4H_9N_3O_2$) and leucine ($C_6H_{13}NO_2$), with accurate positive ion masses of 132.076 and 132.102, can be distinguished at 4,000 resolution. For isotope tracing, high resolution can distinguish species labeled with different heavy nuclei. For example, M+1

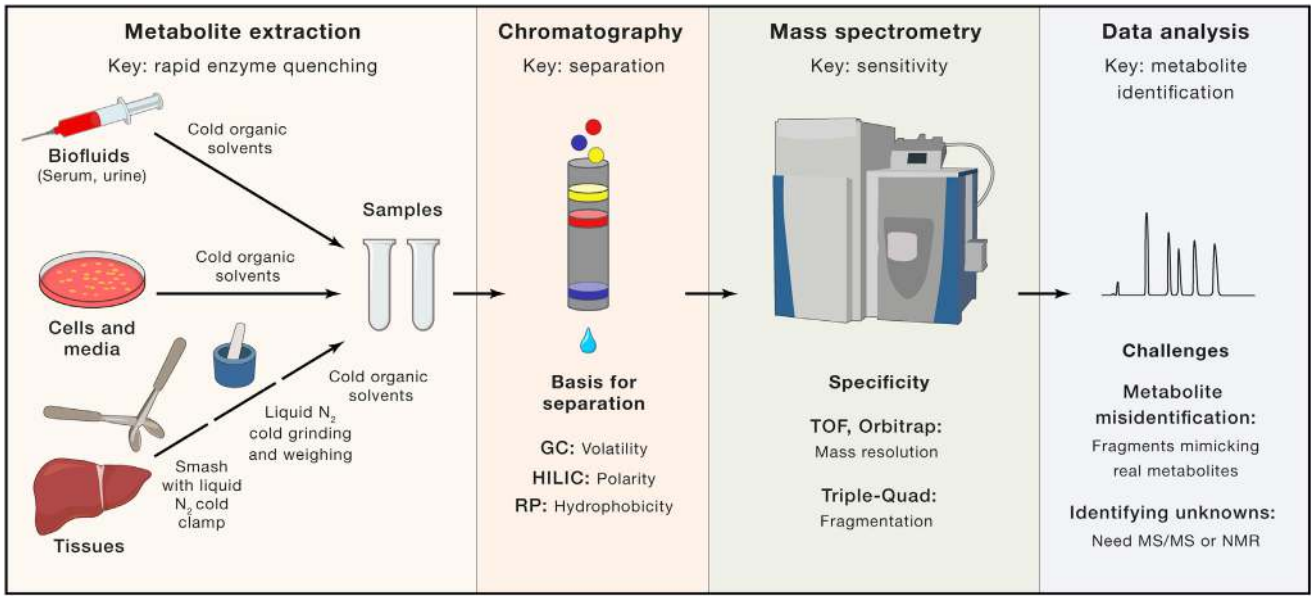

Figure 3. Steps in Metabolomic Analysis
GC, gas chromatography; HILIC, hydrophilic interaction chromatography; RP, reversed phase chromatography.

palmitate isotopologues with one ^{2}H versus one ^{13}C can be separated at 100,000 mass resolution.

To be detected by the MS, a liquid extract must be ionized. This is most commonly done by electrospray ionization: applying high voltage to liquid as it flows out the tip of a needle, thereby converting the liquid into tiny charged droplets that eventually generate gas phase ions (Fenn et al., 1990) (Figure 4A).

Electrospray ionization is a relatively "soft" (i.e., gentle) ionization process which typically yields the intact (de)protonated metabolite ion, $(M+H)^+$ in positive ion mode and $(M-H)^-$ in negative ion mode. It also generates, however, a diversity of adducts (e.g., $[M+Na]^+$) and fragments, which complicate the resulting mass spectra and downstream data analysis.

Common mass analyzers used in metabolomics are time-of-flight (TOF), orbitrap, and quadrupole. All three manipulate ions in electric fields. TOF instruments race ions down a flight tube. First, ions are accelerated through a voltage drop (ΔV) to impart kinetic energy. The ion's velocity then depends on its mass-to-charge ratio (m/z), with lower m/z ions flying faster down the flight tube (Figure 4A). Current TOF instruments typically have mass resolving power of 10,000–60,000 (Junot et al., 2014). Orbitrap instruments monitor ion oscillations up and down a spindle-shaped electrode. Ions are injected into the orbitrap and rotate around the spindle, with electrostatic attraction balanced by centripetal force. Due to the shape of the spindle, the ions also oscillate along its long axis, with the frequency of these z axis oscillations dependent only on ion m/z (Zubarev and Makarov, 2013). The frequency of these oscillations can be used to determine m/z with resolution in excess of 100,000 and even up to 1,000,000. Albeit at greater cost, even higher resolution can be achieved in ion cyclotron resonance instruments in which cyclic ion movement is induced by a strong magnetic field (Marshall et al., 1998).

In contrast to high-resolution mass analyzers like TOF and orbitrap, which can measure all incoming ions, quadrupoles act as low-resolution mass filters, filtering out all ions except those of a particular m/z of interest (±0.5 dalton). Quadruples are commonly placed in front of high-resolution mass analyzers to make a hybrid mass spectrometer such as a quadruple time-of-flight (Q-TOF). This enables isolation of ions of a particular mass followed by their fragmentation (by collision with inert gas) and high-resolution analysis of the fragment ions. The resulting tandem MS (MS/MS) spectra reflect the structure of the parent ion and can be used for metabolite identification (Figure 4D). Alternatively, quadruples can be placed in series in the absence of a high-resolution mass analyzer to make a triple quadruple instrument. Triple quadrupoles measure only a predefined targeted subset of ions but offer the best sensitivity for measuring a single analyte.

Chromatography

By physically separating analytes on a column before MS measurement, chromatography enhances metabolome coverage and improves the quantitative accuracy of MS. Chromatography is particularly important due to the competitive nature of the electrospray ionization process; abundant ions suppress the signal of co-ionizing species (Furey et al., 2013). Chromatographic separation reduces ion suppression, improving detection of low-abundance species. It also prevents quantitative artifacts wherein changes in the concentration of an abundant species systematically alter the signal intensity of other co-ionizing metabolites.

Another merit of chromatography is separation of isomers, which are compounds with same molecular formula but different structures, like leucine and isoleucine (Figure 4C). Isomers are common in metabolism. For example, there are more than a dozen isomers of hexose phosphate, each with distinct

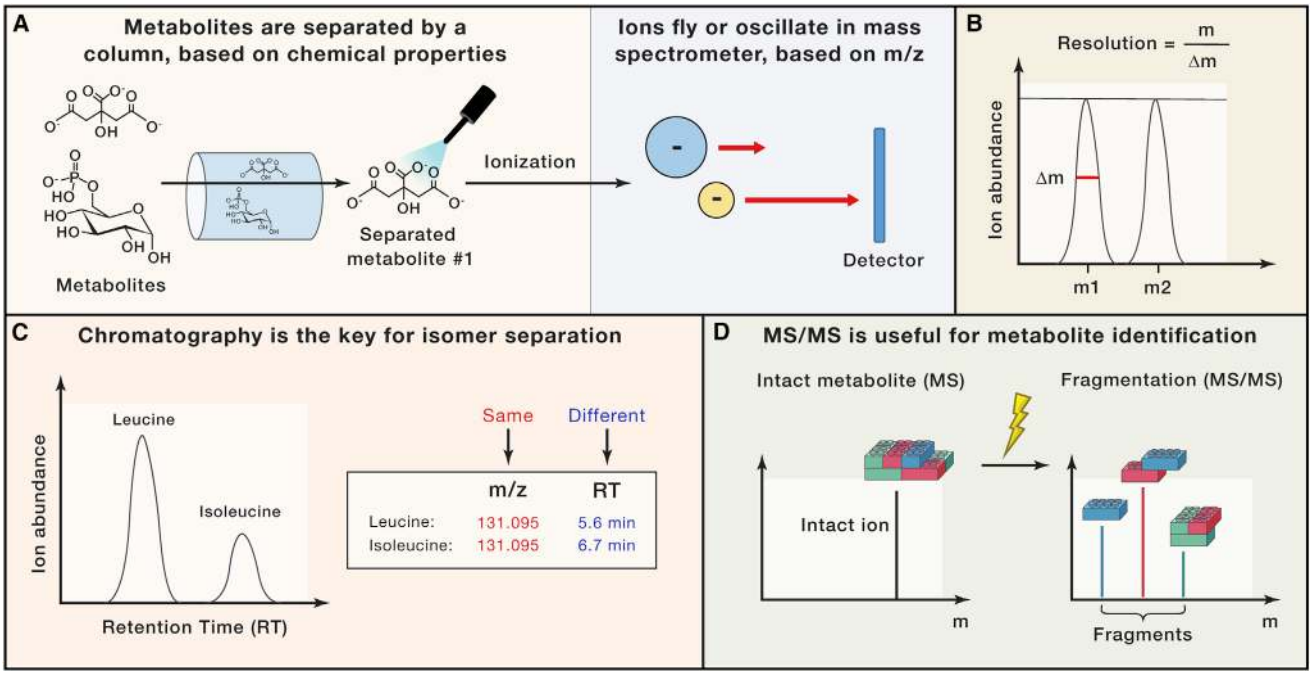

Figure 4. LC-MS Concepts

(A) LC separation is followed by ionization (typically by electrospray) and MS detection. Detector reports signal intensity for specific m/z.

(B) Resolution refers to the ability of the mass spectrometer to distinguish metabolites of similar mass.

(C) Chromatography is crucial for separation of isomers that have same m/z.

(D) MS/MS provides information about chemical moieties within a compound, facilitating metabolite identification.

biological roles. Isomers are indistinguishable by straightforward MS but can be differentiated by chromatography and/or MS/MS fragmentation pattern.

Chromatography is also critical for distinguishing real metabolite signals from imposter signals arising from metabolite fragmentation during the ionization step, where high ionization energy may break down some metabolites into fragments with identical m/z to other metabolites (Xu et al., 2015). For example, citrate fragments mimic four different carboxylic acid metabolites. ATP fragments mimic ADP and AMP. Thus, while direct MS analysis without chromatography can detect a large number of ions with high throughput (Link et al., 2015), it is subject to many false positives and negatives (Lu et al., 2017).

Chromatography and MS are normally coupled together, as gas chromatography-MS (GC-MS) or liquid chromatography-MS (LC-MS). GC requires analytes to vaporize and separates them based on their partitioning between the gas phase (“mobile phase”) and a liquid layer on the chromatography column interior (“stationary phase”). It is most commonly coupled to MS by electron ionization, a hard ionization technique that produces a characteristic set of fragments in lieu of the intact metabolite ion. Peaks can be identified by retention time and matching the fragmentation pattern to spectral libraries. GC has superior chromatographic resolution to LC, with GC-MS particularly good for measuring analytes of low molecular weight (e.g., acetate), high volatility (e.g., alcohols), or poor ionization by electrospray (e.g., sterols). With chemical derivatization, it can also measure medium-sized charged metabolites, like sugar monophosphates (Lai and Fiehn, 2016).

LC separates metabolites based on their partitioning between solvent and micron-sized beads packed within the column. Reversed-phase (RP) chromatography involves hydrophobic beads (typically C18) and elution with a gradient from water to organic solvent. It works well for many polar metabolites and lipids but fails to retain hydrophilic metabolites like amino acids. It also produces poor peak shape for metabolites that contain multiple phosphate groups, such as ATP. These deficiencies can be corrected by adding to the running buffer a moderately hydrophobic cation, like triethylamine, which functions as an ion-pairing agent that helps bind anionic metabolites to the column (Coulier et al., 2006). A cationic-ion-pairing agent, however, causes severe ion suppression in positive mode and can take weeks to rinse out of an LC system; thus, a system dedicated to negative mode analysis is required.

Hydrophilic interaction chromatography (HILIC) involves hydrophilic beads and elution with a gradient from organic solvent to water. HILIC methods have advanced substantially over the past decade and allow positive- and negative-mode analysis to be performed on the same instrument. A diversity of HILIC column chemistries are available (Jandera, 2011). Among these, we find an amide resin to be particularly effective for measuring the core metabolome (Bajad et al., 2006; Yuan et al., 2012). Another type of liquid separation, which is also well suited to measuring the core metabolome, is capillary electrophoresis, where separation is based on differential

voltage-driven movement through liquid rather than on column interactions (Soga et al., 2003).

Data Processing

The first step in data analysis is converting raw MS data into an annotated table indicating peak identities and intensities across samples. This involves computational algorithms that pick peaks, align them across samples, and quantitate peak intensities. Most of the >10,000 peaks found in a typical LC-MS run reflect environmental contaminants, adducts, or in-source fragments, as opposed to metabolite molecular ions, and can be ignored. Interesting peaks fit into one of two categories: (1) they correspond to known metabolites or (2) they differ significantly across biological conditions.

Given a well-annotated chromatography method, known metabolites can be identified based on exact mass and retention time. The open-source Maven software (now maintained as ElMaven) was designed specifically to pull out intensities and labeling patterns of known metabolites peaks (Melamud et al., 2010). Given an accurate library of chromatographic retention times (measured using metabolite standards), Maven or related commercial software enables both easy review of raw ion-specific chromatograms and streamlined processing of these raw data into tables of known metabolites signal intensities.

To find peaks that differ across biological conditions, the open-source program XCMS is widely used (Smith et al., 2006). It identifies significant changes and facilitates searching for MS/MS spectral matches. XCMS can also be accessed online via a web-based platform. Peaks can be identified by matching to retention time and/or fragmentation pattern of known standards. Fragmentation patterns, as measured by MS/MS, are reasonably consistent across instruments, enabling metabolite identification by searching MS/MS spectral databases (e.g., HMDB, METLIN) (Smith et al., 2005; Wishart et al., 2007; Kind et al., 2017). When no MS/MS match is found, MS/MS can nevertheless provide hints regarding the functional groups present in unknown compounds. NMR remains, however, the gold standard for small molecule structure elucidation (Caceres-Cortes and Reily, 2010).

Interpretation

The starting point for interpreting metabolomics data is understanding the relationship between signal intensities and concentrations. In MS, for any given analyte, signal intensity, which is measured in ion counts, generally depends linearly on concentration. Thus, relative amounts can be inferred based on ion count fold change. Across compounds, however, response factors (e.g., ionization efficiency) vary dramatically. Thus, absolute quantitation requires comparison to standards. This is best achieved by adding isotopic internal standards at the time of quenching. Because isotopic standards are not available for many metabolites, it is sometimes easier to label the biological sample (e.g., by growing cells in [U-^{13}C]-glucose) (Bennett et al., 2008; Neubauer et al., 2012; Park et al., 2016). Once absolute metabolite levels are known for a reference condition, absolute levels in other conditions can be determined by relative quantitation. Thinking in terms of concentrations, as opposed to arbitrary signal intensities, helps to contextualize findings. For example, when the metabolite rises in a given condition, is it impacting osmolality? Or is it still present only in trace amounts? How does the concentration relate to the K_m of consuming enzymes?

A good way to visualize the overall pattern of concentration changes in a metabolomics dataset is clustered heatmaps, which can be generated using free open-source tools (e.g., Cluster 3.0 and Java Treeview). Metabolites that show similar patterns across samples group together, as reflected in the dendrogram (tree diagram). Figure 5A shows an example of a clustered heatmap, in this case for an experiment probing the response of whole-cell and mitochondrial-metabolite pools to different respiratory chain inhibitors (Chen et al., 2016). The heatmap nicely illustrates that mitochondrial metabolites respond particularly strongly and variably to the different inhibitors.

Heatmaps can also be used to group together samples that show similar metabolic responses. A more refined way of assessing the overall similarity or differences between samples is principal component analysis, which identifies linear combinations of metabolites that best differentiate samples. Plotting the position of samples along the first two principal components graphically highlights which samples have similar metabolite profiles (Figure 5B). Such plots can be generated by free software like MetaboAnalyst (Xia et al., 2015).

Another aspect of data analysis is to find metabolites (or labeling patterns) that change significantly across conditions. This can be done using standard statistical tests like Student's t test or analysis of variance (ANOVA). Because metabolomics studies measure many metabolites, it is expected that some metabolites will yield a p value < 0.05 based on chance alone (on average 5 out of 100). To reduce the false discovery rate, p values should be adjusted using the Benjamini-Hochberg procedure. Findings that are significant after false discovery correction can be highlighted in bar graphs (Figure 5C).

For isotope tracing, one convenient way to visualize labeling patterns is stacked bar graphs, where each color refers to a particular labeled form. Before analyzing labeling data, it is important to correct for natural isotope abundances. The biggest contributor is the natural carbon 13 abundance of 1.1%, but it is best to correct for all relevant natural isotopes, taking into account the tracer employed and the resolving power of the mass spectrometer. Software exists for this purpose (Midani et al., 2017; Su et al., 2017). Labeling fractions provide complementary information to the absolute magnitude of labeled forms.

After looking at a clustered heatmap and then individually at altered metabolites, key messages in the data often begin to crystalize. To facilitate this process, we routinely "get to know" any unfamiliar metabolite that shows an interesting concentration or labeling change by examining its structure, checking its production and consumption routes using a pathway database like KEGG or MetaCyc (Kanehisa et al., 2016; Caspi et al., 2018), and searching for known biological associations using Google or PubMed. Software has also been developed to help identify significantly affected pathways based on the fraction of pathway metabolites showing altered levels in a particular experiment. For example, in the respiratory chain inhibitor experiment shown in Figure 5, 45 metabolites show 2-fold concentration changes. Pathways enriched in these metabolites can be identified using MetaboAnalyst or other similar software (Figure 5D). Alanine, aspartate, and glutamate metabolism

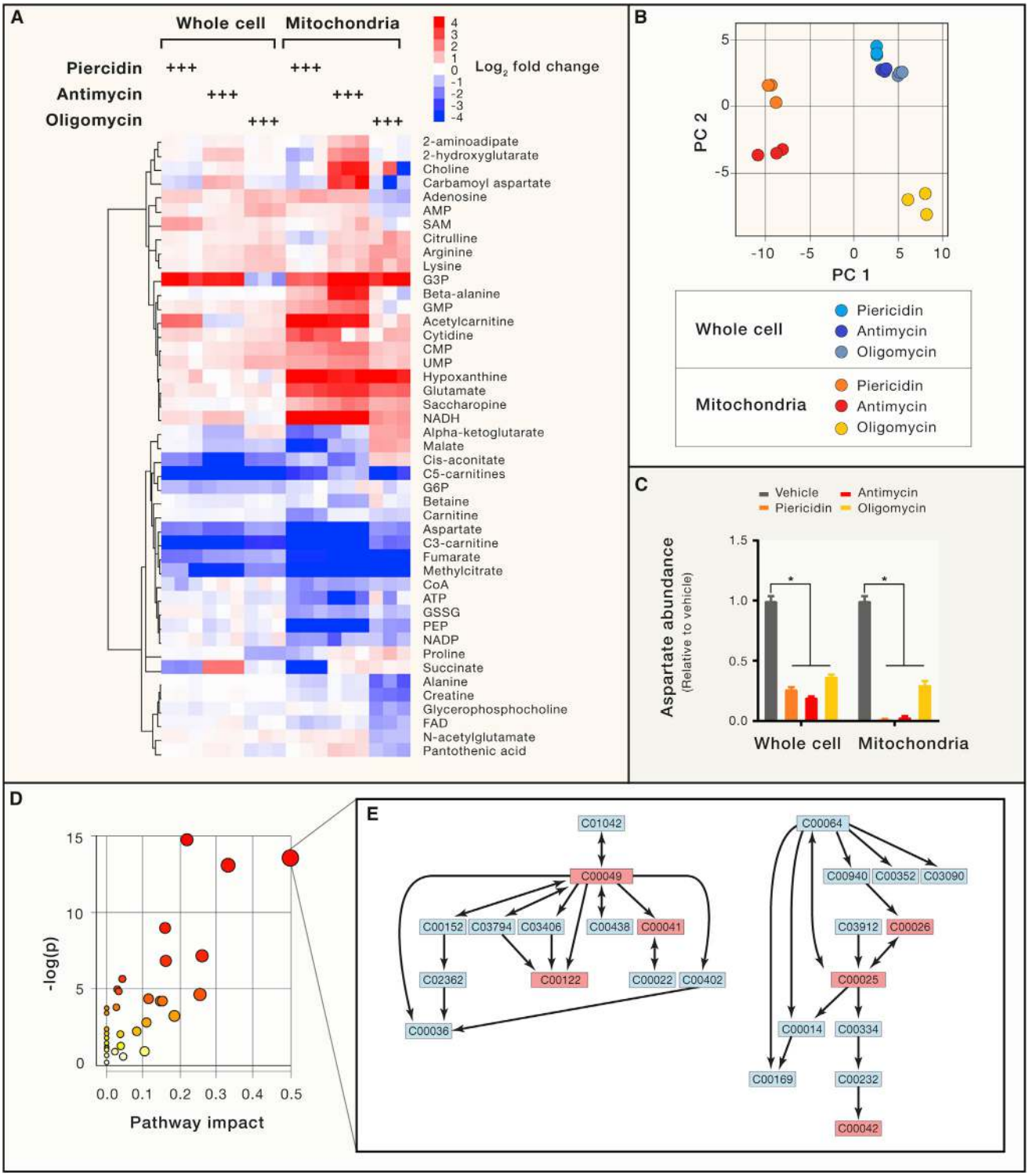

Figure 5. Visualization of a Metabolomics Dataset

The dataset measured whole-cell and mitochondrial matrix metabolome changes in response to three different respiratory chain inhibitors (Chen et al., 2016).
(A) Heatmap of metabolite concentration changes. For simplicity, only metabolites showing 2-fold changes in at least one condition are shown. In practice, we encourage users to examine all metabolites, as those that do not change in concentration can also be informative.
(B) Principle component analysis.

(legend continued on next page)

(KEGG map00250) is one of the top hits (Figure 5E). This example shows the feasibility of pathway analysis but also its current limitations. Alanine, aspartate and glutamate metabolism is not actually a classical pathway, and the KEGG pathway diagram does not illuminate the biochemical basis for the differential responses of the involved metabolites. These data can be rationalized, however, by knowledge of the relationship between the electron transport chain, TCA cycle, and amino acids. This is why we rely heavily on learning metabolic biochemistry, and reading and discussing broadly, as the cornerstones of effective interpretation of metabolomics data.

Biological Application

Here, we highlight four general ways in which metabolomics and isotope tracing can illuminate biology. In each case, we discuss selected successful experiments. The goal is not to review the contributions of metabolomics and isotope tracing but to discuss a small set of experiments with an eye toward inspiring new users.

Finding that Special Metabolite

One of the most powerful applications of metabolomics is finding metabolites with specific biological roles. A straightforward case involves identifying the substrates of enzymes. For novel or promiscuous enzymes, the physiological substrate can be hard to identify biochemically. There are now many examples of successfully employing metabolomics for this purpose. The typical experimental design involves knocking out the enzyme and looking for changes in the metabolome. In most cases, enzyme knockout results in buildup of the physiological substrate, with software like XCMS effective for pulling out these peaks from untargeted MS data (Saghatelian et al., 2004).

Metabolomics can also identify unexpected enzyme products. A particularly important case involved active site mutants of the TCA cycle enzyme isocitrate dehydrogenase (IDH1 and IDH2) that cause human cancer (Parsons et al., 2008). While initial biochemistry hinted that the mutant enzymes were inactive (Zhao et al., 2009), metabolomics analysis revealed that cells expressing oncogenic mutant IDH had a normal amount of the enzyme's typical substrate and product but dramatic increases in three unexpected LC-MS peaks (Dang et al., 2009). These three peaks all occurred at a single retention time, suggesting that they all arose from a single metabolite. One of these peaks proved to be the molecular anion of the metabolic error product, 2-hydroxyglutarate, produced by the mutant enzyme. The other two were the sodium adduct and in-source dehydration product. Subsequent work showed that 2-hydroxyglutarate causes cancer by inhibiting histone and DNA demethylation (Figueroa et al., 2010).

Metabolomics can also be used to identify metabolites associated with more complex biological functions. One approach is to start with an extract that triggers a biological response of interest. Size filtration, organic extraction, or heat can be used to determine whether the activity resides in a small molecule or macromolecule (e.g., protein). When the activity resides in a small molecule, metabolomics can identify those present. The extract can then be purified into fractions, looking for MS (or NMR) peaks that track with the biological activity. This approach was successful in identifying a catabolite of the amino acid valine, 3-hydroxyisobutyrate, as an inducer of fat transport across vascular endothelial cells (Jang et al., 2016).

Perhaps the greatest interest is in identifying metabolites linked to common human diseases for use as diagnostic or prognostic markers. The potential for metabolites to serve this role is well established, with glucose and cholesterol measurements central to modern medicine. Importantly, modest changes in concentration (e.g., 50%) in glucose and cholesterol are used to guide diagnosis and therapy. To find similar biomarkers via metabolomics, large sample sizes are required. To reduce both the effort required for picking peaks and the statistical chance of false discoveries, to date, the most successful metabolomics studies of common human diseases have focused on known metabolites. For example, to discover metabolites that are predictive of type 2 diabetes development, samples of 2,422 individuals followed for 12 years from the Framingham Offspring Study were analyzed by LC-MS, focusing on the core metabolome using triple-quadrupole MS. This revealed that a modest increase (30%) in the concentrations of branched-chain amino acids (BCAAs: leucine, isoleucine, valine) predicts future insulin resistance (Newgard et al., 2009; Wang et al., 2011). Because of the difficulty of proving causation in such population-based human studies, looking for the same phenotype in mouse models is valuable. Indeed, elevated BCAAs were found early in standard mouse diabetes models (Lynch and Adams, 2014). These models are now being used to identify the mechanisms underlying the rise in BCAAs and how such elevation may contribute to pathogenesis. Collectively, these studies highlight the utility of metabolomics in finding metabolites of special biological importance, including new drivers of two of the most common diseases: cancer and diabetes.

Seeing the Big Picture

Beyond finding metabolites of special importance, a key virtue of metabolomics is the global perspective. In many cases, confidence is increased by seeing multiple related metabolites change in parallel. Notable examples include increased levels of all three BCAAs (leucine, isoleucine, and valine) in diabetes (Newgard et al., 2009; Wang et al., 2011) and increased levels of three different nicotinamide-related metabolites in autism (Yap et al., 2010). Similarly, while various acetylated spermidine species had been previously linked to cancer (Tsuji et al., 1975), interest in these metabolites as a biomarker is much increased

(C) Bar graph showing data for a specific metabolite, aspartate. Statistical significance is determined by Student's t test with p values corrected for false discovery rate (FDR) by the Benjamini-Hochberg procedure. *$p < 0.05$.
(D) Identification of impacted metabolic pathways using the MetaboAnalyst software package. Pathways are evaluated on two criteria: Enrichment for metabolites showing at least 2-fold concentration change in one condition (p value based on enrichment by hypergeometric test) and "Pathway impact," a less straightforward measure that takes into account whether the altered metabolites are centrally or peripherally located in the pathway. Circle size is proportional to –log(p) and redness to the pathway impact score. The most "impacted" pathway is alanine, aspartate, and glutamate metabolism (KEGG map00250).
(E) Upon clicking on the dot in (D), the software opens the pathway diagram in (E). Each rectangle is a metabolite with its KEGG ID shown. Altered metabolites are marked in red.

after it emerged as the strongest cancer predictor in multiple metabolomics studies (Johnson et al., 2015; Wikoff et al., 2015).

Beyond putting specific metabolic changes in context, metabolomics can also reveal general biological principles. For example, multiple metabolomics studies in microbes support the concept that metabolism is relatively robust to genetic changes but sensitive to the nutrient environment. In both *E. coli* and yeast, single knockout of an enzyme has only a modest effect on the overall metabolome, mainly accumulation of metabolites directly upstream of the eliminated enzyme (Ishii et al., 2007; Ewald et al., 2013). Knockout mutants of transcription factors and signaling proteins show weaker but broader changes in metabolome, which are relatively subtle but reflective of the gene's function (Mülleder et al., 2016; Fuhrer et al., 2017). In contrast, changes in the nutrient environment lead to large global changes in metabolite concentrations (Ishii et al., 2007; Boer et al., 2010). Why does knockout of a central metabolic enzyme usually produce only focal metabolic changes, while nutrient deprivation produces global ones? The metabolic network contains multiple partially redundant pathways, which can bypass many blockages. But there is no substitute for elemental nutrients. More generally, metabolism is closely tied to the nutrient environment by the strong impact of substrate availability on fluxes (Hackett et al., 2016). Big metabolite changes in response to nutrient limitation may have a diversity of benefits: providing a robust intracellular signal of the nutrient conditions; optimizing survival and growth in the difficult nutrient environment; and preparing the cell for rapid recovery when nutrient conditions improve (You et al., 2013).

Metabolomics can also be integrated with other 'omic approaches (Huan et al., 2017). One important goal of such efforts is to understand regulatory interactions spanning different biomolecule classes. This is often facilitated by dynamic measurements. For example, serial metabolomic and transcriptomic measurements of plant responses to light/dark cycling in *Arabadopsis* identified that darkness quickly induces protein-degradation genes (Caldana et al., 2011). This is followed by increases in amino acid levels. The increased levels of amino acids in turn triggers downregulation of amino acid biosynthetic genes. Such 'omics-driven hypothesis generation is valuable, with the ultimate proof lying in confirmatory genetic experiments testing cause and effect.

Tracking Pathways in Action

Metabolomics measures metabolite abundances. While informative, metabolite abundances do not reveal pathway activities: metabolite levels are determined by the balance of production and consumption in a nonlinear way. Increased metabolite levels can be due to either faster production or slower consumption. Differentiating these alternatives is often critical. For example, when the production of a metabolite is enhanced in a disease state, then it is logical to inhibit the pathway. Accordingly, there is great value in probing pathway fluxes with isotope tracers.

This can be achieved by introducing the tracer and measuring the dynamics of downstream metabolite labeling. Intuitively, faster labeling implies higher flux. Indeed, for a metabolite made directly from the tracer, initial rate of label accumulation (measured in molarity or moles per cell, not labeling fraction) equals the reaction's flux. For such metabolites, assuming metabolic steady state, flux can also be calculated from the labeling half-time and metabolite pool size: flux = ln 2 × pool size / $t^{1/2}$. For metabolites further downstream, however, labeling dynamics depend on both the flux and the pool size of all metabolites between the tracer and the measured analyte (Figures 6A–6C). For example, glycolysis and the PPP often label at similar rates, mirroring glucose-6-phosphate labeling, despite glycolysis having much higher flux.

An alternative approach involves determining labeling patterns at isotopic steady state. Such experiments advantageously avoid the need to take measurements at many different time points. For example, to evaluate flux through the PPP relative to glycolysis, it is more effective to use steady-state labeling from positionally labeled glucose, than dynamic labeling from [U-^{13}C]-glucose. One effective tracer is glucose labeled selectively at carbons 1 and 2 ([1,2-^{13}C]glucose). Catabolism of this tracer via the oxidative PPP, but not glycolysis, can produce M+1 labeled glycolytic metabolites (Figure 6D). Because the natural isotope M+1 signal is substantial, proper correction for natural isotope abundance is critical. In addition, it is important to be precise in relating the labeling patterns to pathway activities. For example, [1,2-^{13}C]glucose specifically probes the flux from ribose-5-phosphate generated by the oxidative PPP, back into glycolysis via the non-oxidative PPP (Figure 6D). If the ribose is used for nucleotide synthesis, as occurs in proliferating cells, there is no M+1 signature in glycolysis. Table 2 provides a list of tracers and heuristics for interpreting the resulting labeling patterns. It includes simple and widely used methods like feeding uniformly ^{13}C-labeled nutrients and determining their relative contributions to TCA intermediates, as well as clever ways of probing specific fluxes with positionally labeled tracers. As the field of flux analysis matures, we hope that such heuristics will become increasingly well validated and widely used.

For the moment, there continues to be great value in carefully thinking through the atom transformations involved in metabolic pathways, and how they relate to observed labeling patterns. Such analysis can identify unexpected fluxes of biological significance. An important example involves M+5-labeling of citrate in mammalian cells fed [U-^{13}C]glutamine (Figure 6D). The standard metabolic route of glutamine metabolism, involving its conversion to α-ketoglutarate, followed by oxidative metabolism of α-ketoglutarate in the TCA cycle, produces M+4 citrate. In contrast, reductive carboxylation of α-ketoglutarate produces M+5 citrate (Yoo et al., 2008; Mullen et al., 2011; Metallo et al., 2011). This "backwards" TCA flux was rigorously proven by tracing with glutamine labeled selectively at its first carbon ([1-^{13}C]glutamine), and eventually by showing loss of the M+5 citrate upon knockout of IDH1. As such efforts more completely map the functional capacity of metabolism, isotope tracing will become more turnkey for the broader biology community.

Tracing in Multicellular Organisms

In flux analysis, the immediate frontier is tracing in live animals. This is a blast from the past – isotope tracers have been employed in plants and animals from the very beginning of biochemistry – but such studies are being revisited now with the power of metabolomics. Interpretation is more complicated than for cell culture studies or isolated microbes, as labeling in any given tissue reflects not only the average labeling of its

Table 2. Isotopic Tracers for Measuring Pathway Activities

Application	Tracer	Metabolite readouts	Interpretation
Pentose phosphate pathway (PPP)			
PPP overflow	[1,2-^{13}C]glucose	Lactate M+1, M+2	Flux through the combined oxidative and non-oxidative PPP generates M+1 lactate from [1,2-^{13}C]glucose, while glycolysis generates only M+2 lactate (Lee et al., 1998). LacM+1 / LacM+2 reflects ratio of PPP overflow to glycolysis.
Source of ribose (oxidative versus non-oxidative branch of PPP)	[1,2-^{13}C]glucose	Ribose phosphate M+1, M+2	The oxPPP make M+1 ribose phosphate; the non-oxPPP makes M+2. Ratio of M+1/M+2 depends on the gross flux (net flux + exchange flux) of each branch: Reversibility of the non-oxPPP can make M+2 even if all net ribose production is by oxPPP.
Glycolysis, TCA and gluconeogenesis			
Glycolytic rate	[U-^{13}C]glucose	FBP Dihydroxyacetone phosphate 3-phosphoglycerate	Higher flux yields faster labeling. Labeling results should be confirmed by glucose uptake and lactate excretion measurements.
Reversibility of glycolysis	50%: 50% mix of [U-^{12}C]: [U-^{13}C] glucose	Glucose-6-phosphate M+3 FBP M+3	Feeding a mixture of labeled and unlabeled glucose results in unlabeled and M+3 triose phosphates. Reversibility of aldolase produces M+3 FBP. Fructose bisphosphatase activity yields M+3 glucose-6-phosphate (Park et al., 2016).
Gluconeogenesis	[U-^{13}C]lactate [U-^{13}C]glutamine	Glucose M+2, M+3 Glucose-6-phosphate M+2, M+3 3-phosphoglycerate M+2, M+3	Lactate and glutamine are major TCA feedstocks. Flux from TCA to glycolysis catalyzed by PEPCK results in triose phosphate labeling. Fructose bisphosphatase activity then makes labeled hexose phosphates.
Pyruvate carboxylase contribution to TCA	[3-^{13}C]glucose [1-^{13}C]pyruvate	Aspartate M+1 Malate M+1	C1 of pyruvate comes from glucose C3/C4. Pyruvate C1 is lost in making acetyl-CoA, but can enter TCA via pyruvate carboxylase which makes M+1 oxaloacetate and thus M+1 aspartate and M+1 malate (Sellers et al., 2015).
Reductive carboxylation ("backwards" TCA flux)	[U-^{13}C]glutamine [1-^{13}C]glutamine	Citrate M+5, Malate M+3 or Citrate M+1, Malate M+1	Reductive carboxylation of α-ketoglutarate (derived from labeled glutamine) produces M+5 citrate from [U-^{13}C]glutamine and M+1 citrate from [1-^{13}C]glutamine, and subsequent ATP citrate lyase produces M+3 or M+1 malate, respectively (Yoo et al., 2008)
TCA carbon sources	[U-^{13}C]nutrients	Succinate Malate Citrate α-ketoglutarate	Carbon enrichment (number of ^{13}C atoms versus total carbon atoms) reflects carbon contribution from the nutrient; useful *in vivo* with correction for circulating nutrient enrichment (Davidson et al., 2016; Faubert et al., 2017; Hui et al., 2017)
Biosynthesis			
Acetyl-CoA sources	[U-^{13}C]glucose [U-^{13}C]glutamine [U-^{13}C]acetate	Fatty acids (saponified) Acetyl amino acids	Fatty acids (e.g., palmitate) are made from stochastic condensation of labeled and unlabeled acetyl-CoA. Acetyl group labeling can be inferred by binomial fitting of fatty acid labeling or by comparing steady-state labeling of acetyl-amino acids and the corresponding free amino acids.
De novo fatty acid biosynthesis	$^{2}H_2O$	Fatty acids (saponified)	$^{2}H_2O$ labels newly synthesized fat directly and via NADPH, with 21 potential deuterium per palmitate (Lee et al., 1994; Zhang et al., 2017).

(*Continued on next page*)

Table 2. ***Continued***

Application	Tracer	Metabolite readouts	Interpretation
Purine biosynthesis	[U-^{13}C]glycine	ATP M+2 GTP M+2	Purine ring contains a glycine moiety. Newly synthesized purines are M+2.
Pyrimidine biosynthesis	[U-^{13}C]bicarbonate [U-^{15}N]glutamine [U-^{13}C]glutamine	UTP UDP-glucose	Pyrimidines are made from carbonyl phosphate (which contains one bicarbonate and one glutamine nitrogen) and aspartate (which typically contains glutamine nitrogen and carbon (Strong et al., 1983).
Protein synthesis	$^{2}H_2O$ [U-^{13}C]essential amino acids	Amino acids (hydrolyzed from protein)	^{2}H from $^{2}H_2O$ incorporates into non-essential amino acids (Busch et al., 2006). Essential AA are directly incorporated.
One-carbon metabolism			
De novo synthesis of serine	[U-^{13}C]glucose	Serine M+3	Serine is made from glucose via the glycolytic intermediate 3-phosphoglycerate. Fraction of serine M+3 indicates fraction serine made by *de novo* synthesis (Locasale et al., 2011)
Source of folate 1C units	[3-^{13}C]serine [U-^{13}C]glycine [U-^{13}C]sarcosine [U-^{13}C]formate	dTTP M+1 ATP M+1, M+2, M+3, M+4 Formyl-methionine M+1 Formate M+1	dTTP contains a 1C unit from cytosolic methylene-THF. Purine rings contain two 1C units from cytosolic formyl-THF. Formyl-methionine contains a 1C unit from mitochondrial formyl-THF. Excess 1C units are secreted as formate (Ducker et al., 2016). Note that purine rings also contain an intact glycine; thus, ATP M+2 may be from glycine not 1C.
Location of serine catabolism to make cytosolic 1C units	[2,3,3-^{2}H]serine	dTTP M+1, M+2	Direct cytosolic production of methylene-THF by SHMT1 yields dTTP M+2. The more circuitous route from mitochondrial SHMT2 yields dTTP M+1 (Herbig et al., 2002; Ducker et al., 2016).
Methylation through SAM	[Methyl-^{13}C,$^{2}H_3$] methionine	Methylated lysine (free or on histones)	Histones are methylated by SAM with the methyl group from methionine (Zee et al., 2010).
Redox metabolism			
NADH production from GAPDH	[4-^{2}H]glucose	NADH M+1 Lactate M+1 (compare to NAD, pyruvate)	GAPDH transfers the ^{2}H of glyceraldehyde-3-phosphate, derived from [4-^{2}H]glucose, to NADH. The ^{2}H can then be transferred to lactate by LDH (Lewis et al., 2014).
NADPH sources	[1-^{2}H]glucose [3-^{2}H]glucose [4-^{2}H]glucose [2,3,3-^{2}H]serine	NADPH (compare to NADP) Fatty acids (saponified) 2-hydroxyglutarate	The oxPPP makes NADPH from [1-^{2}H]glucose (G6PD) and [3-^{2}H]glucose (PGD) (Fan et al., 2014). Malic enzyme and isocitrate dehydrogenase make NADPH from malate and isocitrate, which can be labeled indirectly via [4-^{2}H]glucose (Liu et al., 2016). Folate metabolism makes NADPH from ^{2}H-serine. ^{2}H can be transferred to fatty acids or 2-hydroxyglutarate (whose production can be induced by mutant IDH expression) (Lewis et al., 2014).
Hydrogen-deuterium exchange between NADPH and water	$^{2}H_2O$	NADPH (compare to NADP) Fatty acids (saponified)	NADPH redox-active hydrogen undergoes water exchange catalyzed by Flavin enzymes. Knowledge of the fraction of NADPH undergoing exchange is required to determine the quantitative contribution of the oxPPP and other NADP reduction pathways (Zhang et al., 2017).
Glutathione biosynthesis	[U-^{13}C]glycine [U-^{13}C]glutamine	Glutathione	Glutathione is made from glutamate, cysteine, and glycine. Glutamine is a main source of glutamate (Mak et al., 2017).

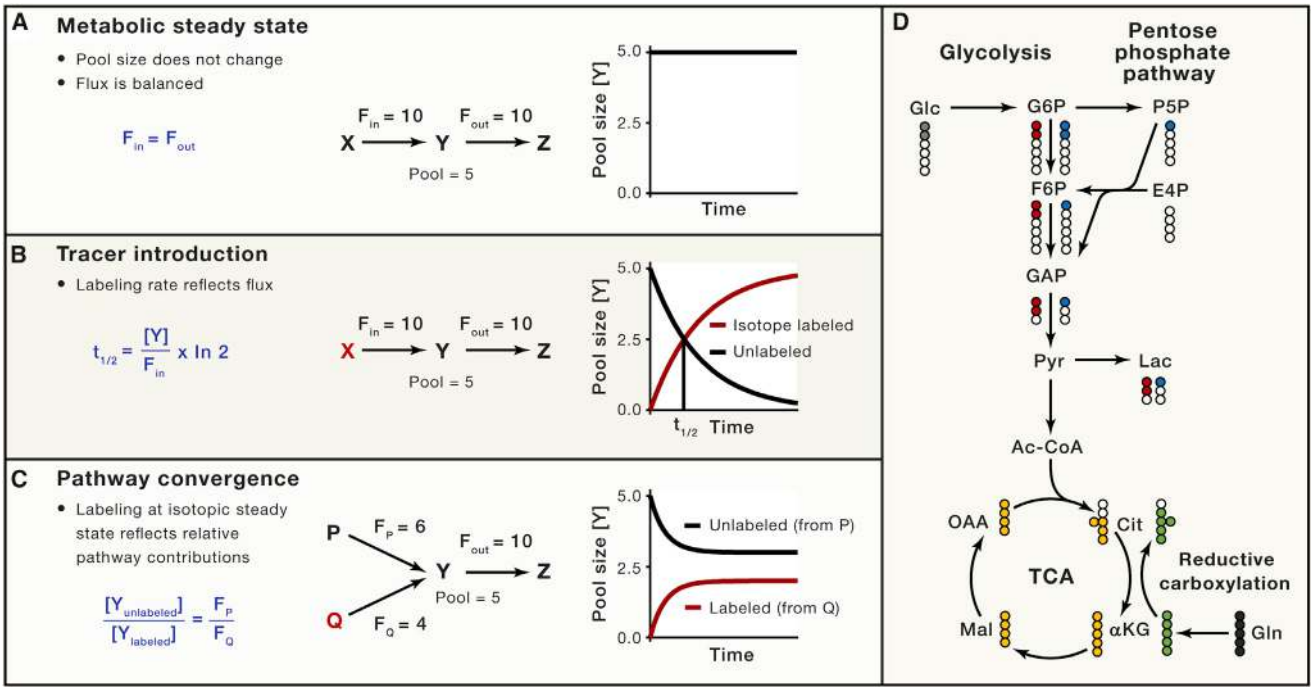

Figure 6. Isotope Tracing to Probe Metabolic Activity

(A–C) Relationship between labeling patterns and flux. X, Y, Z, P, and Q represent metabolites. Arrows represent reactions with F_{in} and F_{out} the fluxes (reaction rates) making and consuming Y, respectively. Graphs reflect pool size of different labeled forms of Y. (A) Based on the law of mass conservation, at metabolic steady state, flow into and out of metabolite pools must balance. (B) Upon instantaneous switching of X from unlabeled to fully labeled, Y becomes labeled over time with single exponential kinetics. Despite the isotope labeling, if no other conditions change, the cells remain at metabolic steady state with constant pool sizes and fluxes. Labeling kinetics depend on both pool size and flux, as shown in the equation. (C) Now consider a case where Y can be produced by two different reactions, using substrates P and Q, with P unlabeled and Q labeled. At isotopic steady state, the unlabeled versus labeled pool size of Y reveals the relative flux from the two different pathways.

(D) Atom mapping for [1,2-^{13}C]glucose tracing pentose phosphate pathway flux and for [U-^{13}C]-glutamine tracing TCA flux. White balls are ^{12}C atoms. Shaded balls are ^{13}C atoms. Glycolysis, red; pentose phosphate pathway, blue; classical TCA turning, yellow; reductive carboxylation, green.

component cells, but also the tracer's pharmacokinetics, i.e., the circuiting levels of the tracer and its metabolites.

To deal with this complexity, some relatively simple calculations are valuable. For animal studies, one key variable is the tracer infusion rate. The required rate of tracer infusion to achieve a particular target enrichment in the circulation can be determined based on knowledge of the circulating nutrient's endogenous production and consumption rates, which at steady state must balance and are termed the nutrient's circulatory turnover flux (F_{circ}) (Hui et al., 2017): $F_{circ} = R(1 - L)/L$, where R is the infusion rate and L the plasma metabolite labeling. It is generally advantageous to achieve enrichment in the range of 10%–30%, to minimize perturbation of circulating metabolite levels while having enough tracer on board to see labeling of downstream products.

Another useful measurement is the fractional contribution of a circulating nutrient to downstream tissue metabolite levels. For example, how much does glutamine contribute to the TCA cycle? This can be probed by infusing labeled glutamine until steady-state tissue labeling is achieved. To estimate glutamine's TCA contribution, the simplest approach is to divide the tissue TCA intermediate labeling by the serum glutamine labeling. This approach works well when the nutrient is mainly catabolized within a tissue. For glutamine, it has revealed that, despite its dominant contribution to the TCA cycle in cultured cancer cells (DeBerardinis et al., 2007), it is a minority contributor for tumors *in vivo* (Hensley et al., 2016; Davidson et al., 2016). When the infused nutrient can also feed tissues indirectly, via transformation into another circulating metabolite, a more sophisticated approach is needed. To identify the direct contribution of different nutrients, it is necessary to conduct tracer experiments with all of the circulating nutrients of interest (e.g., glucose, lactate, and glutamine). Given data on the labeling of each circulating nutrient by each tracer, as well as tissue labeling data, the direct contributions of each nutrient can then be determined by a straightforward matrix calculation. Using this approach, we have found that TCA labeling from infused glucose mainly occurs via circulating lactate: Certain cells break glucose down into lactate, which is secreted into the circulation and used as a primary TCA substrate for most tissues and even for tumors (Faubert et al., 2017; Hui et al., 2017). In this manner, glycolysis and the TCA cycle are uncoupled in individual tissues, enabling their independent tissue-specific regulation. Thus, tracing in animals can reveal new design principles of organismal metabolism.

Future Directions

An important direction in metabolomics is standardization of analytical procedures (Salek et al., 2015). This addresses several needs. First, while the individual steps of analysis are not

especially complicated, building an effective integrative workflow remains tricky. Second, standardization of chromatography is needed to enable effective sharing across laboratories of peak identities. Well-vetted libraries of exact mass and retention time should eventually enable automated quantitation of known metabolites. Standardized procedures should also include posting of annotated data tables, including measured masses, retention times, and individual sample peak intensities, to public repositories. With continuous improvements in instrumentation, standardization of protocols, and automation of data analysis and sharing, metabolomics is poised to be increasingly broadly available and useful to biologists over the coming decade.

What are the frontiers? One immediate need is better understanding the scope of metabolites. There is a vast gulf between the ~200 water-soluble metabolites that many labs now routinely measure, and the ~10,000 peaks that are found in a typical LC-MS run. Most of this difference is the result of individual metabolites producing many different ions, due to adduct formation and in-source fragmentation (Mahieu and Patti, 2017). After accounting for these phenomena, however, there may still be more unknown than identified metabolites.

A longer term goal is to capture the spatial organization of metabolism. Genetically encoded fluorescent metabolite reporters provide an unmatched combination of spatial and temporal resolution and are amenable to live imaging. Effective reporters are available, however, for only a few metabolites. A promising alternative is imaging MS (Bodzon-Kulakowska and Suder, 2016). Since there is no chromatographic step to separate isomers and in-source degradation products, a key challenge in imaging MS is ensuring accurate peak identification. Current methods have a spatial resolution of about 20 μm, which is sufficient to assess metabolite levels in different tissue and tumor regions, but not across subcellular organelles. To determine organellar metabolite levels, an auspicious approach is rapid organelle purification, which is facilitated by genetically encoding an affinity tag on the organelle of interest (Chen et al., 2016). Metabolomics can then be performed as for any other sample. Users need to be mindful of the potential for metabolite alterations, either due to continued enzymatic activity or metabolite leakage during the purification process.

Imaging MS and organelle purification will both be most valuable in combination with isotope tracing. A key opportunity is to use multiple tracers and measurement methods to reveal metabolic activity across tissues, cell types, and intracellular organelles. A major challenge will be making sense of the data. Graphical representation of labeling patterns and intuitive data interpretation is likely to continue to be important, but, as complexity increases, mathematical modeling may become more central to driving biological discovery. This Primer explicitly does not discuss large-scale quantitative flux analysis, because it currently relies on modeling that is beyond the capacity of most labs. Development of software that makes quantitative flux analysis broadly accessible is an important goal. For such efforts to maximize their impact, they must ultimately allow flux determination in multi-compartment systems, including organs connected via the circulation. Combined progress in experimental and computational methods hold the potential to produce a picture of metabolism in action, in space and time. The resulting knowledge should inform many of society's greatest challenges, from green technology to cancer therapy.

ACKNOWLEDGMENTS

We thank Uwe Sauer, Gina Lee, Shogo Wada, and members of the Rabinowitz lab for comments and suggestions. This work was supported by funding from the US National Institutes of Health (R01CA163591, P30CA072720, DP1DK113643, P30DK019525) and Department of Energy (DE-SC0018420, DE-SC0018260). C.J. is a postdoctoral fellow of the American Diabetes Association (1-17-PDF-076).

DECLARATION OF INTERESTS

The authors declare no competing interests.

REFERENCES

Bajad, S.U., Lu, W., Kimball, E.H., Yuan, J., Peterson, C., and Rabinowitz, J.D. (2006). Separation and quantitation of water soluble cellular metabolites by hydrophilic interaction chromatography-tandem mass spectrometry. J. Chromatogr. A *1125*, 76–88.

Beckonert, O., Keun, H.C., Ebbels, T.M.D., Bundy, J., Holmes, E., Lindon, J.C., and Nicholson, J.K. (2007). Metabolic profiling, metabolomic and metabonomic procedures for NMR spectroscopy of urine, plasma, serum and tissue extracts. Nat. Protoc. *2*, 2692–2703.

Bennett, B.D., Yuan, J., Kimball, E.H., and Rabinowitz, J.D. (2008). Absolute quantitation of intracellular metabolite concentrations by an isotope ratio-based approach. Nat. Protoc. *3*, 1299–1311.

Bodzon-Kulakowska, A., and Suder, P. (2016). Imaging mass spectrometry: Instrumentation, applications, and combination with other visualization techniques. Mass Spectrom. Rev. *35*, 147–169.

Boer, V.M., Crutchfield, C.A., Bradley, P.H., Botstein, D., and Rabinowitz, J.D. (2010). Growth-limiting intracellular metabolites in yeast growing under diverse nutrient limitations. Mol. Biol. Cell *21*, 198–211.

Busch, R., Kim, Y.-K., Neese, R.A., Schade-Serin, V., Collins, M., Awada, M., Gardner, J.L., Beysen, C., Marino, M.E., Misell, L.M., and Hellerstein, M.K. (2006). Measurement of protein turnover rates by heavy water labeling of nonessential amino acids. Biochim. Biophys. Acta *1760*, 730–744.

Caceres-Cortes, J., and Reily, M.D. (2010). NMR spectroscopy as a tool to close the gap on metabolite characterization under MIST. Bioanalysis *2*, 1263–1276.

Caldana, C., Degenkolbe, T., Cuadros-Inostroza, A., Klie, S., Sulpice, R., Leisse, A., Steinhauser, D., Fernie, A.R., Willmitzer, L., and Hannah, M.A. (2011). High-density kinetic analysis of the metabolomic and transcriptomic response of Arabidopsis to eight environmental conditions. Plant J. *67*, 869–884.

Caspi, R., Billington, R., Fulcher, C.A., Keseler, I.M., Kothari, A., Krummenacker, M., Latendresse, M., Midford, P.E., Ong, Q., Ong, W.K., et al. (2018). The MetaCyc database of metabolic pathways and enzymes. Nucleic Acids Res. *46* (D1), D633–D639.

Chen, W.W., Freinkman, E., Wang, T., Birsoy, K., and Sabatini, D.M. (2016). Absolute quantification of matrix metabolites reveals the dynamics of mitochondrial metabolism. Cell *166*, 1324–1337.e11.

Coulier, L., Bas, R., Jespersen, S., Verheij, E., van der Werf, M.J., and Hankemeier, T. (2006). Simultaneous quantitative analysis of metabolites using ion-pair liquid chromatography-electrospray ionization mass spectrometry. Anal. Chem. *78*, 6573–6582.

Dang, L., White, D.W., Gross, S., Bennett, B.D., Bittinger, M.A., Driggers, E.M., Fantin, V.R., Jang, H.G., Jin, S., Keenan, M.C., et al. (2009). Cancer-associated IDH1 mutations produce 2-hydroxyglutarate. Nature *462*, 739–744.

Davidson, S.M., Papagiannakopoulos, T., Olenchock, B.A., Heyman, J.E., Keibler, M.A., Luengo, A., Bauer, M.R., Jha, A.K., O'Brien, J.P., Pierce, K.A., et al. (2016). Environment impacts the metabolic dependencies of Ras-driven non-small cell lung cancer. Cell Metab. *23*, 517–528.

DeBerardinis, R.J., Mancuso, A., Daikhin, E., Nissim, I., Yudkoff, M., Wehrli, S., and Thompson, C.B. (2007). Beyond aerobic glycolysis: transformed cells can engage in glutamine metabolism that exceeds the requirement for protein and nucleotide synthesis. Proc. Natl. Acad. Sci. USA *104*, 19345–19350.

Dietmair, S., Timmins, N.E., Gray, P.P., Nielsen, L.K., and Krömer, J.O. (2010). Towards quantitative metabolomics of mammalian cells: development of a metabolite extraction protocol. Anal. Biochem. *404*, 155–164.

Domingo-Almenara, X., Montenegro-Burke, J.R., Benton, H.P., and Siuzdak, G. (2018). Annotation: A computational solution for streamlining metabolomics analysis. Anal. Chem. *90*, 480–489.

Ducker, G.S., Chen, L., Morscher, R.J., Ghergurovich, J.M., Esposito, M., Teng, X., Kang, Y., and Rabinowitz, J.D. (2016). Reversal of cytosolic one-carbon flux compensates for loss of the mitochondrial folate pathway. Cell Metab. *23*, 1140–1153.

Ewald, J.C., Matt, T., and Zamboni, N. (2013). The integrated response of primary metabolites to gene deletions and the environment. Mol. Biosyst. *9*, 440–446.

Fan, J., Ye, J., Kamphorst, J.J., Shlomi, T., Thompson, C.B., and Rabinowitz, J.D. (2014). Quantitative flux analysis reveals folate-dependent NADPH production. Nature *510*, 298–302.

Faubert, B., Li, K.Y., Cai, L., Hensley, C.T., Kim, J., Zacharias, L.G., Yang, C., Do, Q.N., Doucette, S., Burguete, D., et al. (2017). Lactate metabolism in human lung tumors. Cell *171*, 358–371.e9.

Fenn, J.B., Mann, M., Meng, C.K., Wong, S.F., and Whitehouse, C.M. (1990). Electrospray ionization–principles and practice. Mass Spectrom. Rev. *9*, 37–70.

Fiehn, O. (2002). Metabolomics–the link between genotypes and phenotypes. Plant Mol. Biol. *48*, 155–171.

Figueroa, M.E., Abdel-Wahab, O., Lu, C., Ward, P.S., Patel, J., Shih, A., Li, Y., Bhagwat, N., Vasanthakumar, A., Fernandez, H.F., et al. (2010). Leukemic IDH1 and IDH2 mutations result in a hypermethylation phenotype, disrupt TET2 function, and impair hematopoietic differentiation. Cancer Cell *18*, 553–567.

Fuhrer, T., Zampieri, M., Sévin, D.C., Sauer, U., and Zamboni, N. (2017). Genomewide landscape of gene-metabolome associations in Escherichia coli. Mol. Syst. Biol. *13*, 907.

Furey, A., Moriarty, M., Bane, V., Kinsella, B., and Lehane, M. (2013). Ion suppression; a critical review on causes, evaluation, prevention and applications. Talanta *115*, 104–122.

Hackett, S.R., Zanotelli, V.R., Xu, W., Goya, J., Park, J.O., Perlman, D.H., Gibney, P.A., Botstein, D., Storey, J.D., and Rabinowitz, J.D. (2016). Systems-level analysis of mechanisms regulating yeast metabolic flux. Science *354*, 6311.

Hensley, C.T., Faubert, B., Yuan, Q., Lev-Cohain, N., Jin, E., Kim, J., Jiang, L., Ko, B., Skelton, R., Loudat, L., et al. (2016). Metabolic heterogeneity in human lung tumors. Cell *164*, 681–694.

Herbig, K., Chiang, E.-P., Lee, L.-R., Hills, J., Shane, B., and Stover, P.J. (2002). Cytoplasmic serine hydroxymethyltransferase mediates competition between folate-dependent deoxyribonucleotide and S-adenosylmethionine biosyntheses. J. Biol. Chem. *277*, 38381–38389.

Huan, T., Forsberg, E.M., Rinehart, D., Johnson, C.H., Ivanisevic, J., Benton, H.P., Fang, M., Aisporna, A., Hilmers, B., Poole, F.L., et al. (2017). Systems biology guided by XCMS Online metabolomics. Nat. Methods *14*, 461–462.

Hui, S., Ghergurovich, J.M., Morscher, R.J., Jang, C., Teng, X., Lu, W., Esparza, L.A., Reya, T., Le Zhan, Yanxiang Guo, J., et al. (2017). Glucose feeds the TCA cycle via circulating lactate. Nature *551*, 115–118.

Hung, Y.P., Albeck, J.G., Tantama, M., and Yellen, G. (2011). Imaging cytosolic NADH-NAD(+) redox state with a genetically encoded fluorescent biosensor. Cell Metab. *14*, 545–554.

Ishii, N., Nakahigashi, K., Baba, T., Robert, M., Soga, T., Kanai, A., Hirasawa, T., Naba, M., Hirai, K., Hoque, A., et al. (2007). Multiple high-throughput analyses monitor the response of E. coli to perturbations. Science *316*, 593–597.

Jandera, P. (2011). Stationary and mobile phases in hydrophilic interaction chromatography: a review. Anal. Chim. Acta *692*, 1–25.

Jang, C., Oh, S.F., Wada, S., Rowe, G.C., Liu, L., Chan, M.C., Rhee, J., Hoshino, A., Kim, B., Ibrahim, A., et al. (2016). A branched-chain amino acid metabolite drives vascular fatty acid transport and causes insulin resistance. Nat. Med. *22*, 421–426.

Johnson, C.H., Dejea, C.M., Edler, D., Hoang, L.T., Santidrian, A.F., Felding, B.H., Ivanisevic, J., Cho, K., Wick, E.C., Hechenbleikner, E.M., et al. (2015). Metabolism links bacterial biofilms and colon carcinogenesis. Cell Metab. *21*, 891–897.

Junot, C., Fenaille, F., Colsch, B., and Bécher, F. (2014). High resolution mass spectrometry based techniques at the crossroads of metabolic pathways. Mass Spectrom. Rev. *33*, 471–500.

Kanehisa, M., Sato, Y., Kawashima, M., Furumichi, M., and Tanabe, M. (2016). KEGG as a reference resource for gene and protein annotation. Nucleic Acids Res. *44* (D1), D457–D462.

Kind, T., Tsugawa, H., Cajka, T., Ma, Y., Lai, Z., Mehta, S.S., Wohlgemuth, G., Barupal, D.K., Showalter, M.R., Arita, M., and Fiehn, O. (2017). Identification of small molecules using accurate mass MS/MS search. Mass Spectrom. Rev. https://doi.org/10.1002/mas.21535.

Lai, Z., and Fiehn, O. (2016). Mass spectral fragmentation of trimethylsilylated small molecules. Mass Spectrom. Rev. https://doi.org/10.1002/mas.21518.

Larive, C.K., Barding, G.A., Jr., and Dinges, M.M. (2015). NMR spectroscopy for metabolomics and metabolic profiling. Anal. Chem. *87*, 133–146.

Lee, W.N., Bassilian, S., Ajie, H.O., Schoeller, D.A., Edmond, J., Bergner, E.A., and Byerley, L.O. (1994). In vivo measurement of fatty acids and cholesterol synthesis using D2O and mass isotopomer analysis. Am. J. Physiol. *266*, E699–E708.

Lee, W.-N.P., Boros, L.G., Puigjaner, J., Bassilian, S., Lim, S., and Cascante, M. (1998). Mass isotopomer study of the nonoxidative pathways of the pentose cycle with [1,2-13C2]glucose. Am. J. Physiol. *274*, E843–E851.

Lewis, C.A., Parker, S.J., Fiske, B.P., McCloskey, D., Gui, D.Y., Green, C.R., Vokes, N.I., Feist, A.M., Vander Heiden, M.G., and Metallo, C.M. (2014). Tracing compartmentalized NADPH metabolism in the cytosol and mitochondria of mammalian cells. Mol. Cell *55*, 253–263.

Link, H., Fuhrer, T., Gerosa, L., Zamboni, N., and Sauer, U. (2015). Real-time metabolome profiling of the metabolic switch between starvation and growth. Nat. Methods *12*, 1091–1097.

Liu, L., Shah, S., Fan, J., Park, J.O., Wellen, K.E., and Rabinowitz, J.D. (2016). Malic enzyme tracers reveal hypoxia-induced switch in adipocyte NADPH pathway usage. Nat. Chem. Biol. *12*, 345–352.

Locasale, J.W., Grassian, A.R., Melman, T., Lyssiotis, C.A., Mattaini, K.R., Bass, A.J., Heffron, G., Metallo, C.M., Muranen, T., Sharfi, H., et al. (2011). Phosphoglycerate dehydrogenase diverts glycolytic flux and contributes to oncogenesis. Nat. Genet. *43*, 869–874.

Looger, L.L., Lalonde, S., and Frommer, W.B. (2005). Genetically encoded FRET sensors for visualizing metabolites with subcellular resolution in living cells. Plant Physiol. *138*, 555–557.

Lowry, O.H., Carter, J., Ward, J.B., and Glaser, L. (1971). The effect of carbon and nitrogen sources on the level of metabolic intermediates in Escherichia coli. J. Biol. Chem. *246*, 6511–6521.

Lu, W., Su, X., Klein, M.S., Lewis, I.A., Fiehn, O., and Rabinowitz, J.D. (2017). Metabolite Measurement: Pitfalls to Avoid and Practices to Follow. Annu. Rev. Biochem. *86*, 277–304.

Lu, W., Wang, L., Chen, L., Hui, S., and Rabinowitz, J.D. (2018). Extraction and quantitation of nicotinamide adenine dinucleotide redox cofactors. Antioxid. Redox Signal. *28*, 167–179.

Lynch, C.J., and Adams, S.H. (2014). Branched-chain amino acids in metabolic signalling and insulin resistance. Nat. Rev. Endocrinol. *10*, 723–736.

Mahieu, N.G., and Patti, G.J. (2017). Systems-level annotation of a metabolomics data set reduces 25000 features to fewer than 1000 unique metabolites. Anal. Chem. *89*, 10397–10406.

Mak, T.W., Grusdat, M., Duncan, G.S., Dostert, C., Nonnenmacher, Y., Cox, M., Binsfeld, C., Hao, Z., Brüstle, A., Itsumi, M., et al. (2017). Glutathione primes T cell metabolism for inflammation. Immunity *46*, 675–689.

Mancuso, A., Beardsley, N.J., Wehrli, S., Pickup, S., Matschinsky, F.M., and Glickson, J.D. (2004). Real-time detection of 13C NMR labeling kinetics in perfused EMT6 mouse mammary tumor cells and betaHC9 mouse insulinomas. Biotechnol. Bioeng. *87*, 835–848.

Markley, J.L., Brüschweiler, R., Edison, A.S., Eghbalnia, H.R., Powers, R., Raftery, D., and Wishart, D.S. (2017). The future of NMR-based metabolomics. Curr. Opin. Biotechnol. *43*, 34–40.

Marshall, A.G., Hendrickson, C.L., and Jackson, G.S. (1998). Fourier transform ion cyclotron resonance mass spectrometry: a primer. Mass Spectrom. Rev. *17*, 1–35.

Melamud, E., Vastag, L., and Rabinowitz, J.D. (2010). Metabolomic analysis and visualization engine for LC-MS data. Anal. Chem. *82*, 9818–9826.

Metallo, C.M., Gameiro, P.A., Bell, E.L., Mattaini, K.R., Yang, J., Hiller, K., Jewell, C.M., Johnson, Z.R., Irvine, D.J., Guarente, L., et al. (2011). Reductive glutamine metabolism by IDH1 mediates lipogenesis under hypoxia. Nature *481*, 380–384.

Midani, F.S., Wynn, M.L., and Schnell, S. (2017). The importance of accurately correcting for the natural abundance of stable isotopes. Anal. Biochem. *520*, 27–43.

Mülleder, M., Calvani, E., Alam, M.T., Wang, R.K., Eckerstorfer, F., Zelezniak, A., and Ralser, M. (2016). Functional metabolomics describes the yeast biosynthetic regulome. Cell *167*, 553–565.e12.

Mullen, A.R., Wheaton, W.W., Jin, E.S., Chen, P.H., Sullivan, L.B., Cheng, T., Yang, Y., Linehan, W.M., Chandel, N.S., and DeBerardinis, R.J. (2011). Reductive carboxylation supports growth in tumour cells with defective mitochondria. Nature *481*, 385–388.

Neubauer, S., Haberhauer-Troyer, C., Klavins, K., Russmayer, H., Steiger, M.G., Gasser, B., Sauer, M., Mattanovich, D., Hann, S., and Koellensperger, G. (2012). U13C cell extract of Pichia pastoris–a powerful tool for evaluation of sample preparation in metabolomics. J. Sep. Sci. *35*, 3091–3105.

Newgard, C.B., An, J., Bain, J.R., Muehlbauer, M.J., Stevens, R.D., Lien, L.F., Haqq, A.M., Shah, S.H., Arlotto, M., Slentz, C.A., et al. (2009). A branched-chain amino acid-related metabolic signature that differentiates obese and lean humans and contributes to insulin resistance. Cell Metab. *9*, 311–326.

O'Brien, E.J., Monk, J.M., and Palsson, B.O. (2015). Using genome-scale models to predict biological capabilities. Cell *161*, 971–987.

Overmyer, K.A., Thonusin, C., Qi, N.R., Burant, C.F., and Evans, C.R. (2015). Impact of anesthesia and euthanasia on metabolomics of mammalian tissues: studies in a C57BL/6J mouse model. PLoS ONE *10*, e0117232.

Park, J.O., Rubin, S.A., Xu, Y.F., Amador-Noguez, D., Fan, J., Shlomi, T., and Rabinowitz, J.D. (2016). Metabolite concentrations, fluxes and free energies imply efficient enzyme usage. Nat. Chem. Biol. *12*, 482–489.

Parsons, D.W., Jones, S., Zhang, X., Lin, J.C., Leary, R.J., Angenendt, P., Mankoo, P., Carter, H., Siu, I.M., Gallia, G.L., et al. (2008). An integrated genomic analysis of human glioblastoma multiforme. Science *321*, 1807–1812.

Rabinowitz, J.D., and Kimball, E. (2007). Acidic acetonitrile for cellular metabolome extraction from Escherichia coli. Anal. Chem. *79*, 6167–6173.

Rogers, J.K., and Church, G.M. (2016). Genetically encoded sensors enable real-time observation of metabolite production. Proc. Natl. Acad. Sci. USA *113*, 2388–2393.

Saghatelian, A., Trauger, S.A., Want, E.J., Hawkins, E.G., Siuzdak, G., and Cravatt, B.F. (2004). Assignment of endogenous substrates to enzymes by global metabolite profiling. Biochemistry *43*, 14332–14339.

Salamanca-Cardona, L., Shah, H., Poot, A.J., Correa, F.M., Di Gialleonardo, V., Lui, H., Miloushev, V.Z., Granlund, K.L., Tee, S.S., Cross, J.R., et al. (2017). In vivo imaging of glutamine metabolism to the oncometabolite 2-Hydroxyglutarate in IDH1/2 mutant tumors. Cell Metab. *26*, 830–841.e3.

Salek, R.M., Neumann, S., Schober, D., Hummel, J., Billiau, K., Kopka, J., Correa, E., Reijmers, T., Rosato, A., Tenori, L., et al. (2015). COordination of Standards in MetabOlomicS (COSMOS): facilitating integrated metabolomics data access. Metabolomics *11*, 1587–1597.

Sauer, U. (2006). Metabolic networks in motion: 13C-based flux analysis. Mol. Syst. Biol. *2*, 62.

Sellers, K., Fox, M.P., Bousamra, M., 2nd, Slone, S.P., Higashi, R.M., Miller, D.M., Wang, Y., Yan, J., Yuneva, M.O., Deshpande, R., et al. (2015). Pyruvate carboxylase is critical for non-small-cell lung cancer proliferation. J. Clin. Invest. *125*, 687–698.

Smith, C.A., O'Maille, G., Want, E.J., Qin, C., Trauger, S.A., Brandon, T.R., Custodio, D.E., Abagyan, R., and Siuzdak, G. (2005). METLIN: a metabolite mass spectral database. Ther. Drug Monit. *27*, 747–751.

Smith, C.A., Want, E.J., O'Maille, G., Abagyan, R., and Siuzdak, G. (2006). XCMS: processing mass spectrometry data for metabolite profiling using nonlinear peak alignment, matching, and identification. Anal. Chem. *78*, 779–787.

Soga, T., Ohashi, Y., Ueno, Y., Naraoka, H., Tomita, M., and Nishioka, T. (2003). Quantitative metabolome analysis using capillary electrophoresis mass spectrometry. J. Proteome Res. *2*, 488–494.

Sorge, R.E., Martin, L.J., Isbester, K.A., Sotocinal, S.G., Rosen, S., Tuttle, A.H., Wieskopf, J.S., Acland, E.L., Dokova, A., Kadoura, B., et al. (2014). Olfactory exposure to males, including men, causes stress and related analgesia in rodents. Nat. Methods *11*, 629–632.

Strong, J.M., Anderson, L.W., Monks, A., Chisena, C.A., and Cysyk, R.L. (1983). A 13C tracer method for quantitating de novo pyrimidine biosynthesis in vitro and in vivo. Anal. Biochem. *132*, 243–253.

Su, X., Lu, W., and Rabinowitz, J.D. (2017). Metabolite spectral accuracy on orbitraps. Anal. Chem. *89*, 5940–5948.

Tsuji, M., Nakajima, T., and Sano, I. (1975). Putrescine, spermidine, N-acetylspermidine and spermine in the urine of patients with leukaemias and tumors. Clin. Chim. Acta *59*, 161–167.

Wang, T.J., Larson, M.G., Vasan, R.S., Cheng, S., Rhee, E.P., McCabe, E., Lewis, G.D., Fox, C.S., Jacques, P.F., Fernandez, C., et al. (2011). Metabolite profiles and the risk of developing diabetes. Nat. Med. *17*, 448–453.

Want, E.J., Masson, P., Michopoulos, F., Wilson, I.D., Theodoridis, G., Plumb, R.S., Shockcor, J., Loftus, N., Holmes, E., and Nicholson, J.K. (2013). Global metabolic profiling of animal and human tissues via UPLC-MS. Nat. Protoc. *8*, 17–32.

Wenk, M.R. (2010). Lipidomics: new tools and applications. 143, 888-895.

Wikoff, W.R., Hanash, S., DeFelice, B., Miyamoto, S., Barnett, M., Zhao, Y., Goodman, G., Feng, Z., Gandara, D., Fiehn, O., and Taguchi, A. (2015). Diacetylspermine is a novel prediagnostic serum biomarker for non-small-cell lung cancer and has additive performance with pro-surfactant protein B. J. Clin. Oncol. *33*, 3880–3886.

Winder, C.L., Dunn, W.B., Schuler, S., Broadhurst, D., Jarvis, R., Stephens, G.M., and Goodacre, R. (2008). Global metabolic profiling of Escherichia coli cultures: an evaluation of methods for quenching and extraction of intracellular metabolites. Anal. Chem. *80*, 2939–2948.

Wishart, D.S., Tzur, D., Knox, C., Eisner, R., Guo, A.C., Young, N., Cheng, D., Jewell, K., Arndt, D., Sawhney, S., et al. (2007). HMDB: the Human Metabolome Database. Nucleic Acids Res. *35*, D521–D526.

Wittmann, C., Krömer, J.O., Kiefer, P., Binz, T., and Heinzle, E. (2004). Impact of the cold shock phenomenon on quantification of intracellular metabolites in bacteria. Anal. Biochem. *327*, 135–139.

Wollenberger, A., Ristau, O., and Schoffa, G. (1960). A simple technic for extremely rapid freezing of large pieces of tissue. Pflugers Arch. Gesamte Physiol. Menschen Tiere *270*, 399–412.

Xia, J., Sinelnikov, I.V., Han, B., and Wishart, D.S. (2015). MetaboAnalyst 3.0–making metabolomics more meaningful. Nucleic Acids Res. *43* (W1), W251–W257.

Xu, Y.F., Zhao, X., Glass, D.S., Absalan, F., Perlman, D.H., Broach, J.R., and Rabinowitz, J.D. (2012). Regulation of Yeast Pyruvate Kinase by Ultrasensitive Allostery Independent of Phosphorylation. Mol. Cell *48*, 52–62.

Xu, Y.F., Lu, W., and Rabinowitz, J.D. (2015). Avoiding misannotation of in-source fragmentation products as cellular metabolites in liquid chromatography-mass spectrometry-based metabolomics. Anal. Chem. *87*, 2273–2281.

Yap, I.K., Angley, M., Veselkov, K.A., Holmes, E., Lindon, J.C., and Nicholson, J.K. (2010). Urinary metabolic phenotyping differentiates children with autism from their unaffected siblings and age-matched controls. J. Proteome Res. *9*, 2996–3004.

Yoo, H., Antoniewicz, M.R., Stephanopoulos, G., and Kelleher, J.K. (2008). Quantifying reductive carboxylation flux of glutamine to lipid in a brown adipocyte cell line. J. Biol. Chem. *283*, 20621–20627.

You, C., Okano, H., Hui, S., Zhang, Z., Kim, M., Gunderson, C.W., Wang, Y.P., Lenz, P., Yan, D., and Hwa, T. (2013). Coordination of bacterial proteome with metabolism by cyclic AMP signalling. Nature *500*, 301–306.

Yuan, M., Breitkopf, S.B., Yang, X., and Asara, J.M. (2012). A positive/negative ion-switching, targeted mass spectrometry-based metabolomics platform for bodily fluids, cells, and fresh and fixed tissue. Nat. Protoc. *7*, 872–881.

Zee, B.M., Levin, R.S., Xu, B., LeRoy, G., Wingreen, N.S., and Garcia, B.A. (2010). In vivo residue-specific histone methylation dynamics. J. Biol. Chem. *285*, 3341–3350.

Zhang, Z., Chen, L., Liu, L., Su, X., and Rabinowitz, J.D. (2017). Chemical basis for deuterium labeling of fat and NADPH. J. Am. Chem. Soc. *139*, 14368–14371.

Zhao, S., Lin, Y., Xu, W., Jiang, W., Zha, Z., Wang, P., Yu, W., Li, Z., Gong, L., Peng, Y., et al. (2009). Glioma-derived mutations in IDH1 dominantly inhibit IDH1 catalytic activity and induce HIF-1alpha. Science *324*, 261–265.

Zubarev, R.A., and Makarov, A. (2013). Orbitrap mass spectrometry. Anal. Chem. *85*, 5288–5296.